14 Fundamentals in Shoulder Radiology

Ceylan Colak and Carl S. Winalski

14.1 Introduction

The prevalence of shoulder pain in the general population ranges from 16 to 26% [1, 2]. Shoulder pain has various causes, including rotator cuff disease, adhesive capsulitis or "frozen shoulder," shoulder instability, calcific tendinosis, and osteoarthritis. Overall, rotator cuff disease is the most common cause of shoulder pain, responsible for approximately 65–70% of shoulder pain cases [3]; the prevalence of this condition increases with increasing patient age [4].

Shoulder pathologies can be treated conservatively or surgically, and imaging often helps to guide treatment planning. Common conservative treatments include physiotherapy, nonsteroidal anti-inflammatory drugs (NSAIDs), and therapeutic intra-articular injections. The most common surgical approaches are arthroscopy and open surgery. Imaging can help direct which approach is best in cases of surgery for cuff repair, labral repair, and shoulder arthroplasty (conventional total, reverse total shoulder, or hemiarthroplasty) [5]. When clinicians are determining the appropriate treatment course, preoperative evaluation with imaging is essential. This article reviews normal shoulder anatomy, shoulder pathologies, and the appearance of these conditions on commonly used imaging modalities.

14.2 Plain Radiography

Plain radiography of the shoulder is commonly performed as an initial imaging examination. This modality is useful for diagnosing fractures and dislocations in patients with acute trauma. For those with chronic or nontraumatic shoulder pain, radiography provides an overall assessment of joint status and some diagnoses including arthritis, degenerative changes, chronic cuff tear, and calcific tendinosis.

The standard radiographic shoulder series includes an anteroposterior (AP) projection (Fig. 14.1) with the arm internally and/or externally rotated and other views added to show the specific structures of the shoulder. The Y view is obtained by turning the patient 60° anteriorly and centering the posteroanterior (PA) X-ray beam on the shoulder. This view is usually ordered when a shoulder dislocation is suspected; the Y view is also helpful in identifying fractures of the scapular blade (Fig. 14.2). The axillary view allows for clear visualization of the relationship between the glenoid and the

C. Colak (✉)
Imaging Institute, Cleveland Clinic, Cleveland, OH, USA

C. S. Winalski
Imaging Institute, Cleveland Clinic, Cleveland, OH, USA

Department of Biomedical Engineering, Lerner Research Institute, Cleveland Clinic, Cleveland, OH, USA
e-mail: winalsc@ccf.org

G. Huri et al. (eds.), *Shoulder Arthroplasty*, https://doi.org/10.1007/978-3-030-19285-3_14

Fig. 14.1 AP view radiograph of a normal shoulder. Humeral head overlaps the lateral aspect of the glenoid. The glenohumeral joint space (arrow) can be estimated by measuring from the medial margin of the humeral head and medial margin of the glenoid (dotted lines)

Fig. 14.2 Y view radiograph of a normal shoulder. Humeral head overlaps the glenoid (Y) which is at the center of the "Y" formed by the junction of the scapular body (SB), spine (SS), and base of the coracoid (C)

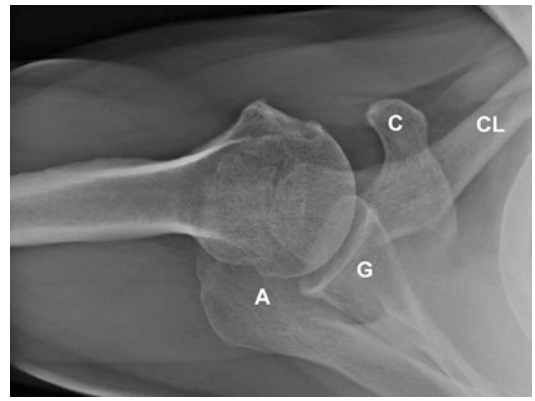

Fig. 14.3 Axillary view radiograph of a normal shoulder. The humeral head is centered on the glenoid (G). The coracoid (C) is anterior. The acromioclavicular joint projects over the humeral head (*A* acromion, *CL* clavicle)

humeral head (Fig. 14.3). This view is acquired with the patient supine, the arm positioned in 90° of abduction, and the X-ray beam centered on the middle of the axilla and angled approximately 30° toward the spine. The Grashey view is obtained by turning the patient 45° posteriorly and using an AP X-ray beam or angling the X-ray beam 45° laterally to the patient. This is a "true" AP view of the glenohumeral joint and is used to show the integrity of the glenohumeral joint without overlapping of the humerus and glenoid (Fig. 14.4). West Point and Velpeau views are variants of the axillary view that are useful in identifying anterior glenoid abnormalities (such as Bankart lesions and posterior dislocations). A West Point view is obtained with the patient prone, the shoulder propped up over the X-ray table, and the arm abducted 90° from the trunk while the hand is pronated; the X-ray beam is angled 25° medially and 25° cephalad. The Velpeau view is commonly used after acute trauma, as it does not require the patient to abduct the arm. The patient sits or stands leaning backward 30° while wearing a sling or Velpeau dressing, and the X-ray beam is directed through the shoulder superoinferiorly. Modified views may need to be obtained when the patient cannot move the arm, particularly in the context of trauma and severe pain.

Fig. 14.4 Grashey radiographic projection is a "true AP" view of the glenohumeral joint obtained with a 35–45° obliquity to show the joint space tangentially. The humeral head should not overlap the glenoid

The medial portion of the humeral head overlaps with the lateral aspect of the glenoid on AP shoulder radiographs, since the glenohumeral joint is anatomically 35–40° oblique to the coronal plane of the patient (Fig. 14.1). In some cases, the humeral head may project slightly lower or slightly higher than the center of the glenoid. Because the humerus is anterior to the glenoid, if the patient is tilted back when the image is taken, the humeral head may appear high relative to the glenoid, whereas if the patient is tilted forward, it may appear slightly low. The distance between the humeral head and acromion should be evaluated. If the humeral head is superiorly subluxed such that the acromiohumeral distance is less than 7 mm, a rotator cuff tear should be suspected. Because the Grashey view is a "true AP" projection of the glenohumeral joint, there should not be any overlap of the humeral head and glenoid on this view. Overlap of these structures on the Grashey view implies subluxation or dislocation of the humeral head. Finally, when reviewing shoulder radiographs, clinicians must also assess the clavicle, scapula, and ribs for fractures and other lesions, as well as the visualized portions of the lungs for any potential pathologies.

Plain radiography is used to diagnose many common shoulder pathologies, including fractures of the humerus, clavicle, and scapula. Proximal humerus fractures are the third most common type of fragility fracture, accounting for nearly 6% of all adult fractures [6, 7]. As the median age of the world's population increases, the incidence of this fracture type has also risen [8]. These fractures and fractures of the midhumerus present few challenges in radiographic interpretation and thus do not usually require further examinations. These fractures present as a lucency and cortical disruption with variable degrees of angulation, impaction, and displacement on plain radiographs (Fig. 14.5). Determining the degrees of angulation and rotation of the fragments may require full-length images of the humerus that include the shoulder and elbow.

Most clavicular fractures are clinically apparent and occur in the midportion or the distal third of the clavicle. In addition, acromioclavicular (AC) joint separation, which is a common traumatic or sports injury, is easily assessed with radiography. The normal AC joint space usually measures <5 mm, and normal coracoclavicular distance is <11–13 mm. Widening of any of these spaces must be considered as a potential separation. AC joint separation is classified into six subgroups based primarily on the distal clavicular angle and degree of the displacement [9]. Some recommend obtaining additional radiographs while hanging weights from the patient's wrists and comparing these images with images of the unaffected side to detect nondisplaced AC joint injuries.

Fractures of the scapula are relatively rare, although they can occur as the result of a severe, direct blow [10]. Because the scapula is a thin bone, fractures of the body of the scapula may be difficult to appreciate. The Velpeau and West Point variants of the axillary view may be useful for evaluation of the scapular spine and acromion, especially for patients with reverse shoulder arthroplasties who are at risk for fracture (Fig. 14.6). When there is any uncertainly regarding the presence or type of fracture on radiography, a computed tomography (CT) scan may be useful.

Shoulder dislocations are readily diagnosed by radiography. Anterior dislocation of the humeral head accounts for more than 95% of shoulder dislocations. On the AP projection, the displaced humeral head will be inferiorly and

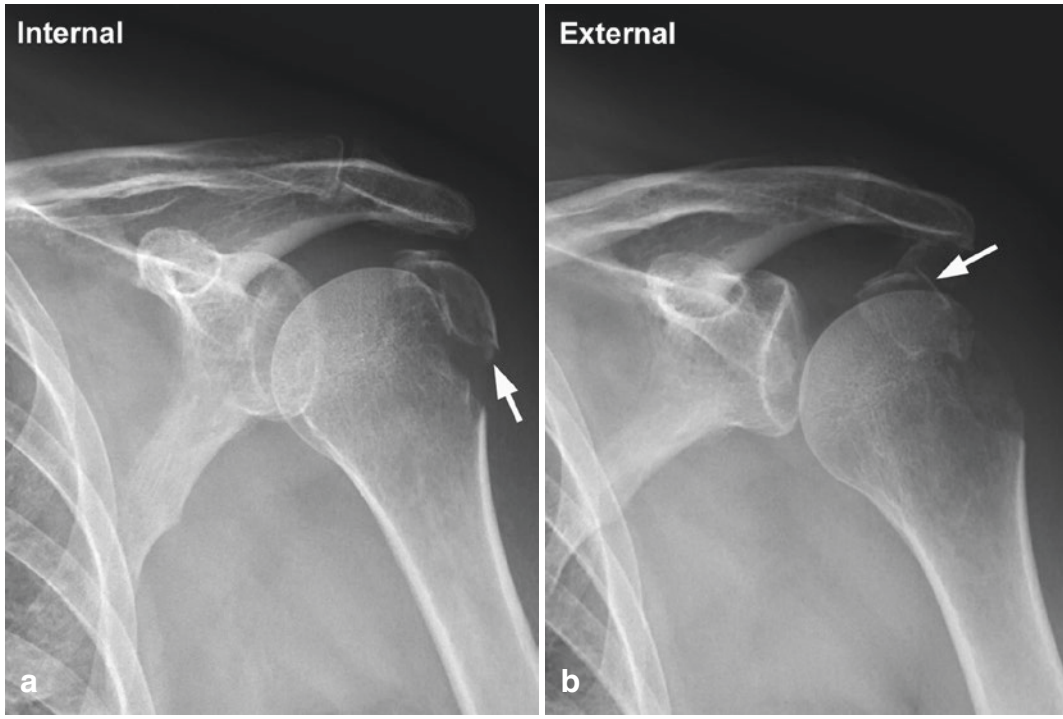

Fig. 14.5 AP radiographs obtained in internal rotation (**a**) and external rotation (**b**) show a displaced fracture of the posterior aspect of the greater tuberosity (arrow)

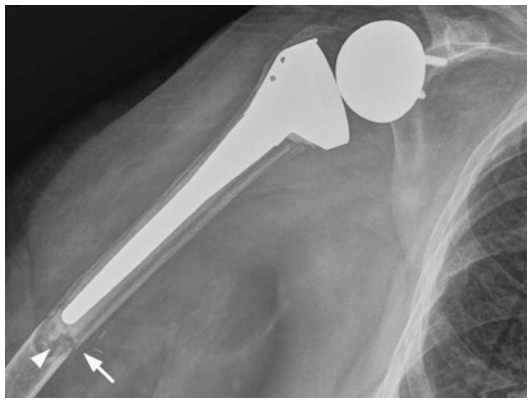

Fig. 14.6 Loosening and periprosthetic fracture following reverse total shoulder arthroplasty. There is lucency around the humeral component with focal osteolysis at the inferior tip (arrowhead). The fracture (arrow) is seen at the tip of the prosthesis

medially displaced, overlapping with the glenoid neck and lying inferior to the coracoid (Fig. 14.7). Impaction of the humeral head on the anterior-inferior edge of the glenoid produces a deformity in the posterolateral portion of the humeral head, the Hill-Sachs deformity, which is best seen on the AP view with the arm internally rotated after reduction of the dislocation. There is often an injury of the anterior inferior glenoid rim, as well; this injury, known as a Bankart lesion, may involve the labrum only or both the labrum and the underlying bone. When there is a bony component, the West Point or axillary view may be diagnostic. When only the soft tissue of the glenoid labrum is involved, magnetic resonance (MR) or CT arthrography will be needed for imaging diagnosis.

Posterior shoulder dislocations are uncommon and more difficult than anterior dislocations to diagnose on a standard AP view of the shoulder. On normal shoulder radiographs using the AP view, there is an overlap of the humeral head and the glenoid with a relatively narrow anterior glenohumeral joint space visible. Radiographs following posterior shoulder dislocation show widening of the glenohumeral joint space; additionally, the humeral head may not appear round because of extreme

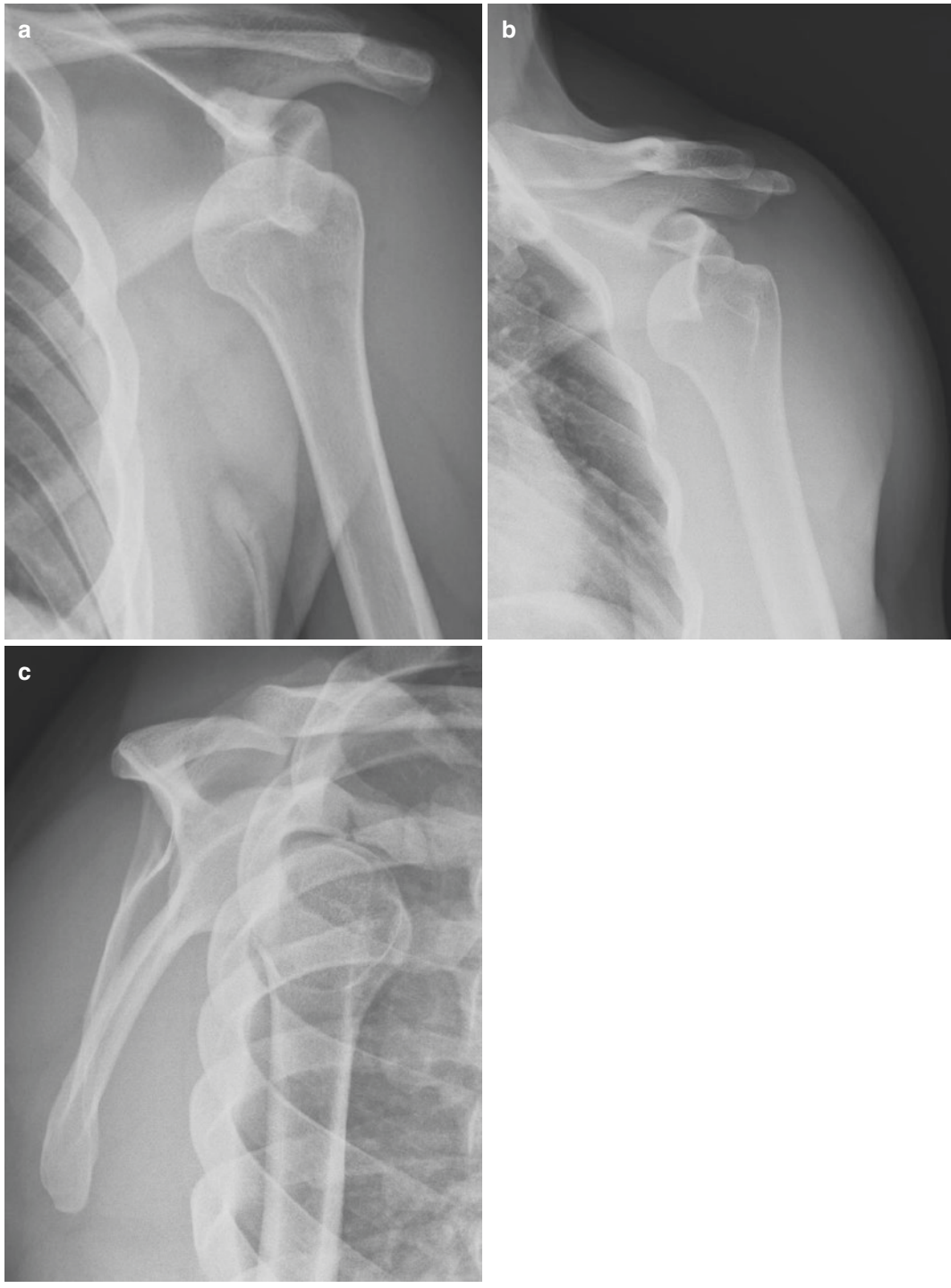

Fig. 14.7 Anterior subcoracoid dislocation. The humeral head overlaps the glenoid on AP (**a**) and Grashey views (**b**). The anterior displacement is well visualized on the Y (**c**) view

internal rotation. On the Grashey view, there will be an abnormal overlap of the humeral head and glenoid. The axillary and Y views will clearly show the posterior dislocation (Fig. 14.8).

Initial evaluation of shoulder arthritis is frequently performed with radiography. Degenerative or post-traumatic osteoarthritis in the shoulder, as with other joints, is frequently associated with osteophyte formation, subarticular sclerosis, subarticular cysts, and joint space narrowing. As the arthritis progresses, there can be loss of the bone stock of the glenoid with alteration of the version of the glenoid face. When planning for shoulder arthroplasty, evaluation of the glenoid version is critical for proper placement of the glenoid component; CT is often performed for this purpose.

Fig. 14.8 Posterior dislocation. Grashey (**a**) and AP internal rotation (**b**) and axillary (**c**) views show the humeral head is reduced, but mildly decentered posteriorly. There is a displaced glenoid fracture fragment (arrowhead) from the posterior articular margin of the glenoid

With septic arthritis of the shoulder, radiographs are typically normal in the early stages, although soft tissue swelling or inferior displacement of the humeral head due to effusion may be seen. With more chronic septic arthritis, radiographs may show decreased bone density, joint space narrowing, and bony destruction. When a septic joint is clinically suspected, joint aspiration should be considered.

Although radiography is not primarily performed for this purpose, radiographic images may be abnormal in the setting of rotator cuff disease. Calcific tendinosis of the rotator cuff (i.e., the deposition of calcific crystals such as hydroxyapatite within an abnormal tendon) can be readily diagnosed on plain radiographs. Typically, this condition presents as amorphous white densities at the greater tuberosity at the insertion of the affected tendon (Fig. 14.9). With large, retracted tears of rotator cuff tendons, the humeral head may migrate superiorly with resultant decentering of the humeral head on the glenoid, thus narrowing the distance between the humeral head and acromion (i.e., the acromiohumeral distance). With time, secondary glenohumeral osteoarthritis, also known as rotator cuff arthropathy, may develop (Fig. 14.10); this condition is suggestive of an irreparable rotator cuff [11].

Bone or soft tissue neoplasms of the shoulder may be initially evaluated or incidentally found on radiography. The proximal humerus is the third most common site for primary bone tumors and soft tissue tumors, with an incidence of approximately 1.8 in 100,000 [12–16]; it is also one of the most common sites of osteosarcoma in children [17]. As with other bone tumor sites, the degree of bone destruction and fracture risk in the shoulder can be estimated with radiographs. However, advanced imaging techniques should be used for further evaluation of potential bone destruction and for identification of soft tissue masses. When an incidental finding of a bone

Fig. 14.9 Calcific tendinosis. Grashey radiograph shows calcifications in the supraspinatus tendon insertion (arrow)

Fig. 14.10 Rotator cuff arthropathy. Grashey radiograph shows superior subluxation of the humeral head with severe narrowing of the subacromial space and remodeling of the inferior acromion indicating a chronic full-thickness rotator cuff tear. Osteophytes and intra-articular bodies indicate concomitant glenohumeral osteoarthritis

lesion (usually an enchondroma) is observed on radiographs, the images should be compared with results from previous imaging studies to determine the biological nature of the abnormality. When a benign lesion is suspected, follow-up radiography is indicated. If an aggressive lesion is suspected on radiographs, MR imaging should be considered.

Although this chapter focuses primarily on preoperative shoulder imaging, there are some important postoperative complications that can be readily evaluated on radiography. Plain radiography is routinely used after shoulder arthroplasty to evaluate implant positioning and baseline appearance for help with future assessment, should symptoms arise. Loosening of an arthroplasty component appears as progressively widening radiolucencies at the bone-implant or cement-bone interface, although plain radiography can sometimes underestimate radiolucent lines [18]. In such cases, CT offers improved sensitivity, especially when metal artifact reduction techniques are implemented. With an infected implant, periosteal reaction may be seen. Scapular notching after reverse total shoulder arthroplasty (i.e., erosion of the scapular neck from impaction of the humeral component) usually occurs within the first few months after surgery. The incidence of scapular notching ranges from 44 to 96% [19, 20], and this condition ranges from grade 1 to 4 in severity (with grade 4 potentially leading to glenosphere loosening) based on radiographic findings. The occurrence of scapular notching may require revision surgery. Therefore, radiographs demonstrating bone loss at the inferior scapular neck should be carefully assessed in patients who have undergone reverse total shoulder arthroplasty (Fig. 14.11). Heterotopic ossification in the triceps origin is common following reverse shoulder arthroplasty (Fig. 14.12). Heterotopic ossification usually does not progress after the initial postoperative period. It usually has no effect on functional movement of the shoulder and usually does not

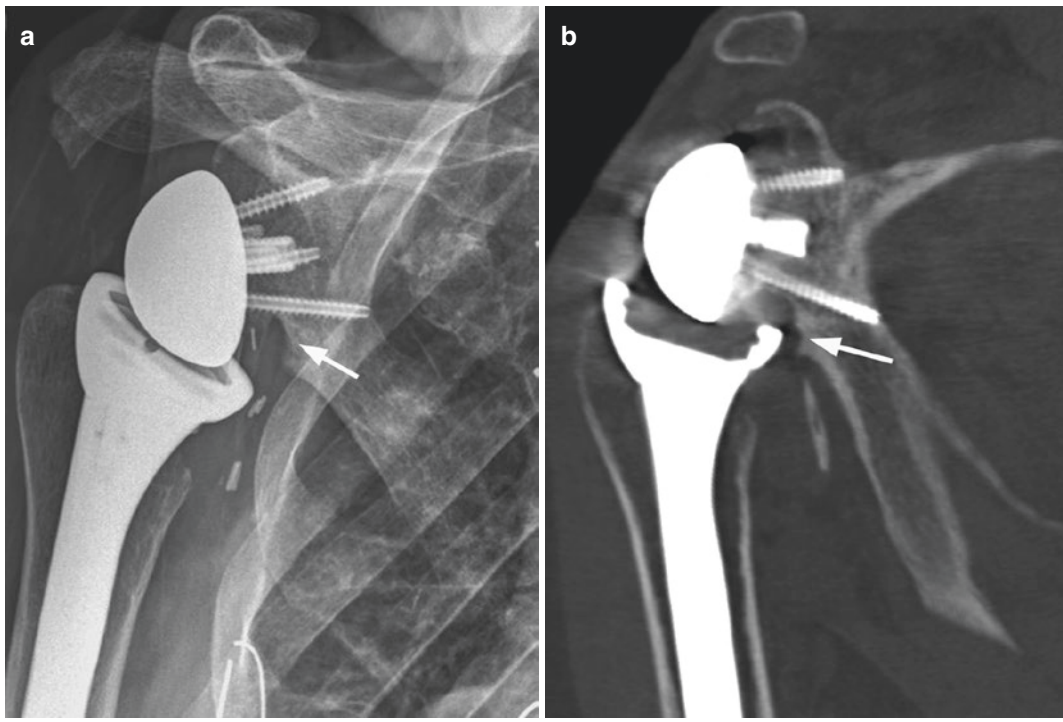

Fig. 14.11 Scapular notching following reverse total shoulder arthroplasty. Grashey radiograph (**a**) shows bone loss (arrow) from the inferior glenoid with exposure of the inferior screw of the glenosphere. The CT (**b**) of the same patient demonstrates the humeral component impacting on the glenoid causing the scapular notching (arrow)

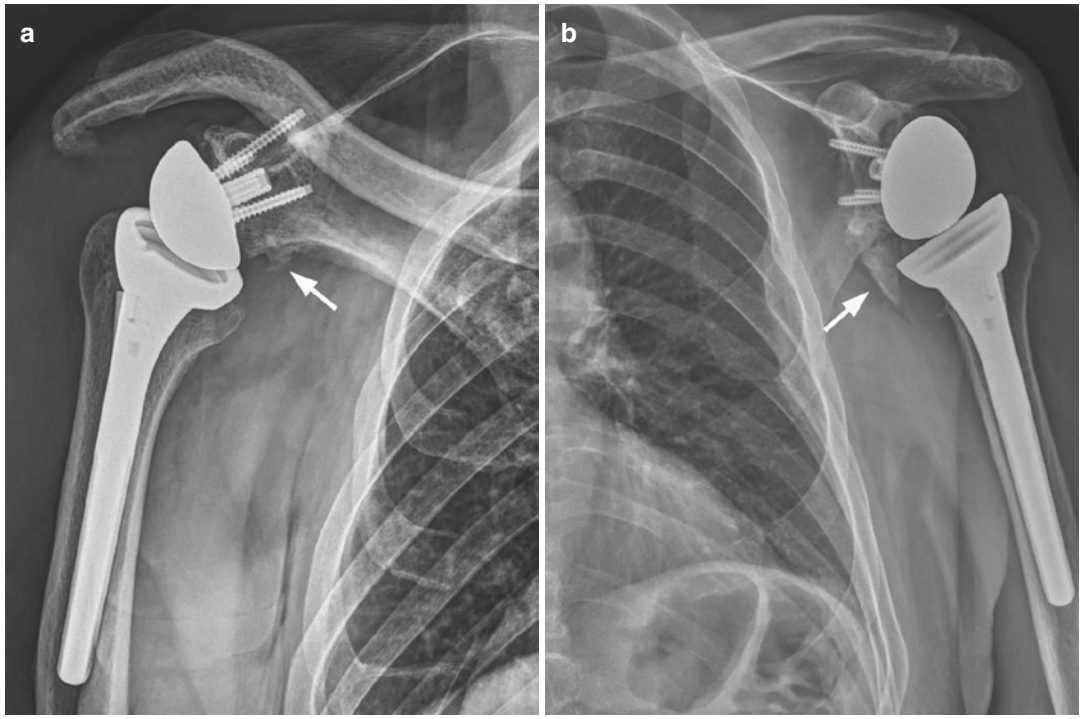

Fig. 14.12 Heterotopic ossifications in (**a**) and (**b**) following reverse total shoulder arthroplasty commonly develop within the triceps extending inferiorly from the scapular neck (arrows). The appearance of heterotopic calcification in (**a**) is differentiated from scapular notching since there is no glenoid bone loss

require treatment. This new bone can mimic scapular notching. However, notching will show loss of glenoid bone, whereas heterotopic ossification is added bone; in addition, notching and heterotopic ossification may coexist [21].

14.3 CT

CT is commonly used in orthopedic imaging to assess cortical bone, trabecular bone, and joint surfaces in patients with fractures, arthritis, shoulder instability, advanced rotator cuff disease, tumors, or infection; however, soft tissue abnormalities are less well visualized by CT than by MR imaging. Because CT is most often obtained with isotropic voxels, 2D multiplanar and 3D reformatted images can be readily created (Fig. 14.13). CT arthrography, which is obtained by injecting iodinated contrast into the shoulder joint before CT imaging is performed, can provide additional information about the articular cartilage, labrum, and rotator cuff. CT

Fig. 14.13 Subcoracoid dislocation. 3D surface rendering reformatted from a CT scan shows the humeral head beneath the coracoid and impacted on the anterior glenoid

arthrography is often used as an alternative for patients who are unable to undergo shoulder MR imaging. CT offers greater spatial resolution than MR imaging, whereas MR imaging offers higher image contrast for soft tissue abnormalities and can demonstrate edema-like signal in the bone marrow [22].

CT can be more effective than radiography in showing the spatial relationship of fracture fragments in complex fractures of the humerus and scapula [23] (Fig. 14.14). Often, radiography is limited in these cases by patient positioning and superimposition of the fracture fragments. Preoperative planning with CT before fracture reduction or in cases of unreducible or recurrent dislocation may be useful. One study of patients with shoulder instability found that preoperative identification and measurement of bony Bankart fragments of the glenoid and Hill-Sachs impaction of the humeral head can be difficult with radiography, leading to challenges in surgical decision-making [24]. Therefore, CT should be considered in the treatment algorithm for accurate quantification of bone loss to prevent a high rate of recurrent shoulder instability. As previously discussed, for patients with severe glenohumeral osteoarthritis, preoperative measurement of the glenoid version with CT is helpful for shoulder arthroplasty planning.

Fig. 14.14 Greater tuberosity fracture. 3D surface rendering reformatted from a CT scan (same patient as Fig. 14.5) demonstrates the displaced fracture (arrow) as well as the cortical defect in the superior lateral aspect of the greater tuberosity (asterisk)

14.4 MR Imaging

Improvements in system hardware and software have led to further reliance on MR imaging for evaluation of the shoulder [25]. This modality provides a thorough overview of both the osseous and soft tissue shoulder structures and has demonstrated a high level of diagnostic accuracy that is improved further with the addition of arthrography [26–28]. Therefore, physicians treating patients with shoulder pathologies must be familiar with shoulder MR imaging.

MR imaging of the shoulder is indicated for the assessment of a wide spectrum of disorders including suspected rotator cuff and biceps tendon tears, intra-articular pathology such as labral tears, articular cartilage defects and underlying bone abnormalities, tumors, and infections. However, the advantages of MR imaging must be weighed against the higher costs and sometimes limited availability of this modality.

14.4.1 Shoulder Anatomy on MR Imaging

The rotator cuff is composed of the tendons of four muscles: the supraspinatus, infraspinatus, subscapularis, and teres minor muscles (Fig. 14.15). The tendons of these muscles attach to the lesser and greater tuberosities of the humerus, with the subscapularis inserting on the lesser tuberosity and the other three tendons inserting on the greater tuberosity [29]. The supraspinatus tendon is best assessed by oblique coronal images that are aligned parallel to the supraspinatus muscle rather than oriented in the true coronal plane. The oblique coronal plane also provides excellent views of the superior and inferior portions of the glenoid labrum as well as the quadrangular and triangular spaces. Oblique

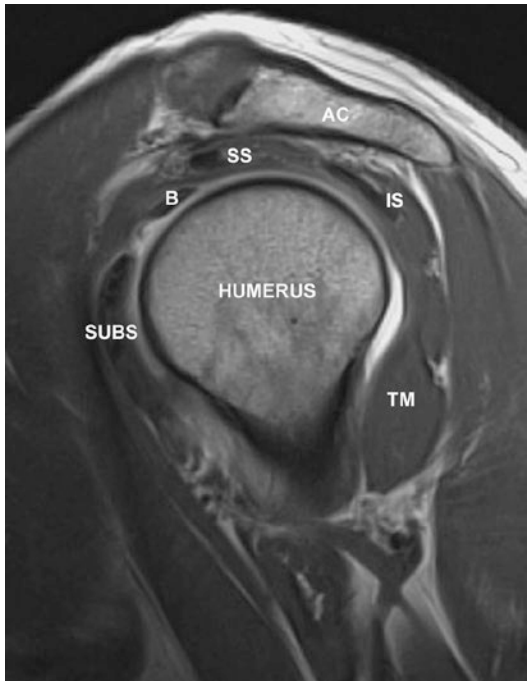

Fig. 14.15 Normal rotator cuff anatomy on a sagittal oblique T1-weighted (T1W) FSE image from an MR arthrogram (*B* biceps, *AC* acromion, *SS* supraspinatus, *SUBS* subscapularis, *IS* infraspinatus, *TM* teres minor)

sagittal images are usually oriented parallel to the glenoid face as seen on axial images and demonstrate the relationship of the rotator cuff tendons with the humeral head (Fig. 14.15). These images provide optimal short-axis views of the rotator cuff tendons and the intra-articular portion of the long head of the biceps tendon. They are particularly helpful for differentiating between nonretracted full-thickness tears and partial-thickness tears and for identifying which tendon(s) is/are involved. These images also help in the evaluation of the glenohumeral ligaments, subacromial-subdeltoid bursa, glenoid labrum, and rotator interval. Axial images are also used to assess the glenohumeral articular cartilage, the anterior and posterior aspects of the labrum, and the subscapularis and biceps tendons.

14.4.2 MR Imaging Protocol

For MR scans, patients are positioned supine with their arm at the side of the body in partial external rotation [25]. A number of different MR imaging protocols have been recommended for evaluation of the shoulder, each of which is effective in showing both normal and pathologic findings. One feature common to these protocols is the acquisition of both fat-suppressed/water-sensitive and non-fat-suppressed fast spin echo (FSE) images. The sequences commonly use echo times (TEs) longer than 35 ms to minimize artifactually bright areas in the tendon from the "magic angle" effect. This magic angle effect occurs when organized collagen fibers, including those in tendons and ligaments, are oriented at 55° to the main magnetic field. T2 relaxation of the tissue is longer, leading to a brighter tendon signal that may mimic tendinosis. Oblique sagittal T1-weighted images are often obtained medial to the spinoglenoid notch to assess fatty infiltration and atrophy of the rotator cuff muscles or to identify edema-like signal that can be seen with muscle denervation resulting from injury or paralabral cysts [29].

Images should be obtained in three planes: oblique coronal, oblique sagittal, and axial. The slice thickness should be less than 5 mm, and a small field of view (FOV) (12–16 cm) is recommended. The glenoid labrum is best seen on high-resolution axial (anterior and posterior labrum) and coronal (superior and inferior labrum) images. Direct MR arthrography (i.e., imaging the joint after intra-articular injection with MR contrast agent) can help to identify articular side partial-thickness cuff tears and can demonstrate nondisplaced labral tears by filling the tears with contrast agent. The advantages of MR arthrography for diagnosing the causes of shoulder instability and SLAP lesions and for the postoperative assessment of labral repairs have been demonstrated previously [30].

14.4.3 MR Imaging of Common Shoulder Pathologies

Early diagnosis of rotator cuff disease is important as untreated disease can result in enlarging tears, increasing pain [31], and irreversible fatty degeneration and atrophy of the cuff muscles [32]. Once these muscle changes occur, the risk

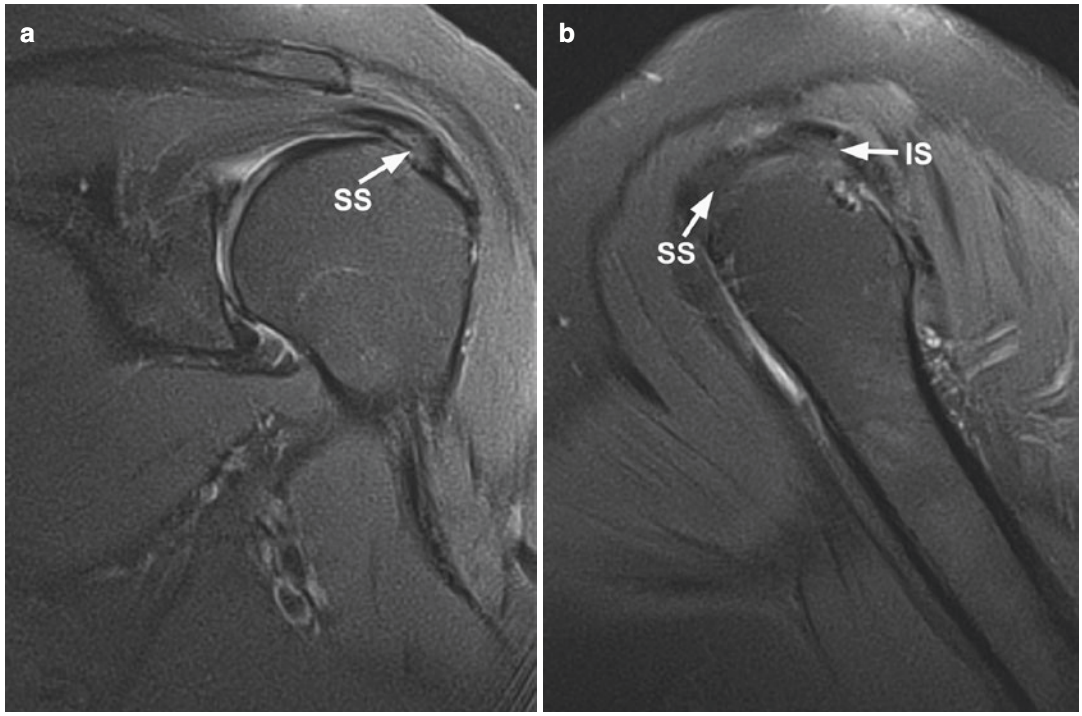

Fig. 14.16 Rotator cuff tendinosis. Coronal (**a**) and sagittal (**b**) oblique T2-weighted (T2W) fast spin echo (FSE) images with fat suppression (fs) show intermediate signal and fusiform swelling in supraspinatus (SS) and infraspinatus (IS) tendon from myxoid degeneration

of a recurrent tear after surgical repair may be as high as 94% [33, 34].

The underlying cause of rotator cuff damage may include shoulder impingement and degenerative arthritis. Patients with uncorrected impingement syndrome may progress along a spectrum from rotator cuff tendinosis to partial-thickness tear to full-thickness tear [34].

MR imaging is effective in assessing rotator cuff pathology, especially full-thickness cuff tears. One study found that with MR imaging, a full-thickness rotator cuff tear could be diagnosed with 92.1% sensitivity and 92.9% specificity; however, MR imaging was less accurate for the diagnosis of a partial-thickness tear with only 63.6% sensitivity (but 91.7% specificity) [35]. On MR images, normal tendons are dark whereas early tendon degeneration (tendinopathy) appears as intermediate signal within the tendon substance accompanied by distortion of the tendon. In the most severe cases, there is fusiform or focal thickening resulting from myxoid degeneration (Fig. 14.16). With more advanced pathology (e.g., partial-thickness tear), the signal becomes brighter on T2-weighted images, and fluidlike signal may be seen across a portion of the tendon. When fluidlike signal traverses the full thickness of the tendon, a full-thickness tear can be diagnosed. In full-thickness tears, retraction of the tendon should be measured, as cases with increasing grades of retraction may require open surgery rather than arthroscopy or may be inoperable (Fig. 14.17).

MR imaging can be very useful in the assessment of patients with shoulder instability. Because only 25–30% of the humeral head contacts the glenoid in the glenohumeral joint, the shoulder has a wide range of motion at the expense of compromised joint stability [36]. The joint is fortified by enlargement of the articular surface by the glenoid labrum and extrinsic components such as the capsule, ligaments, tendons, and muscles. When these components become unbalanced, shoulder instability may occur.

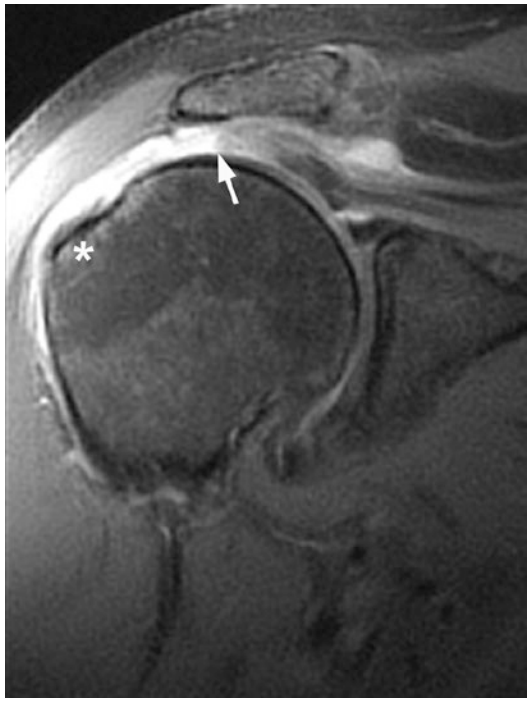

Fig. 14.17 Full-thickness rotator cuff tear. Coronal oblique T2W fs FSE image shows retraction of the torn supraspinatus tendon (arrow) and the empty footplate on the greater tuberosity (asterisk)

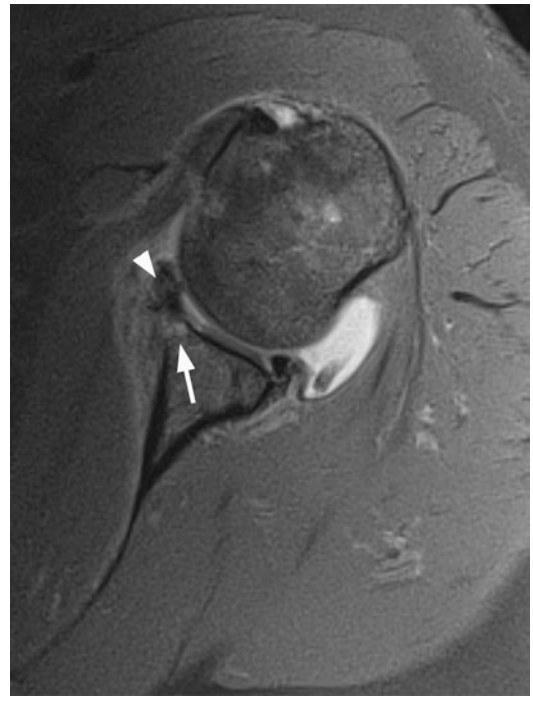

Fig. 14.18 Osseous Bankart lesion. An axial T1W fs FSE image from an MR shoulder arthrogram demonstrates the torn anterior-inferior labrum (arrowhead) and the small glenoid bone defect (arrow) with overlying cartilage damage

Damages to the anterior, inferior, or posterior labrum; the glenoid cartilage; the bony humerus or glenoid; the glenohumeral ligaments; the capsule; the rotator cuff tendons; or the biceps tendons are all potential causes of instability that can be assessed with MR imaging.

Anterior instability is the most common type of shoulder instability. Anterior dislocation usually leads to an injury to the anterior-inferior labrum (i.e., a Bankart lesion) from pulling of the inferior glenohumeral ligament and impaction of the humeral head. Bankart-type injuries may be isolated to the labrum or may include a glenoid bone fragment (i.e., a "bony Bankart") (Fig. 14.18). On MR images, the lesion appears as a high intensity line on T2- or proton density-weighted images coursing through the base of the normally low signal anterior-inferior labrum or beneath the fragment of a bony Bankart lesion. The anterior labrum may remain in place or may appear displaced, small, or absent. The inferior glenohumeral ligament may also pull from its humeral attachment, resulting in a humeral avulsion of the glenohumeral ligament (HAGL) and producing a characteristic appearance on MR images [37, 38]. This HAGL injury is also associated with a tear of the subscapularis tendon and recurrent anterior instability [39]. HAGL lesions typically result from a first-time dislocation in patients aged more than 35 years [38]. On axial MR images, a HAGL lesion appears as a disruption at the humeral neck attachment producing a "J-shaped" rather than the normal "U-shaped" appearance of the inferior glenohumeral ligament (Fig. 14.19).

Anterior dislocations can also cause bony impaction injuries on the posterior-superior humeral head; this is known as a Hill-Sachs deformity. On MR imaging, this lesion appears as focal flattening or a wedge-shaped defect with or without associated bone marrow edema-like signal (Fig. 14.20). Often these deformities are easiest to see on the superior-most axial slices where the

Fig. 14.19 Humeral avulsion of the inferior glenohumeral ligament (HAGL). A coronal oblique T2W fs FSE image shows fluid between the avulsed ligament (arrow) and the expected attachment site on the proximal humerus

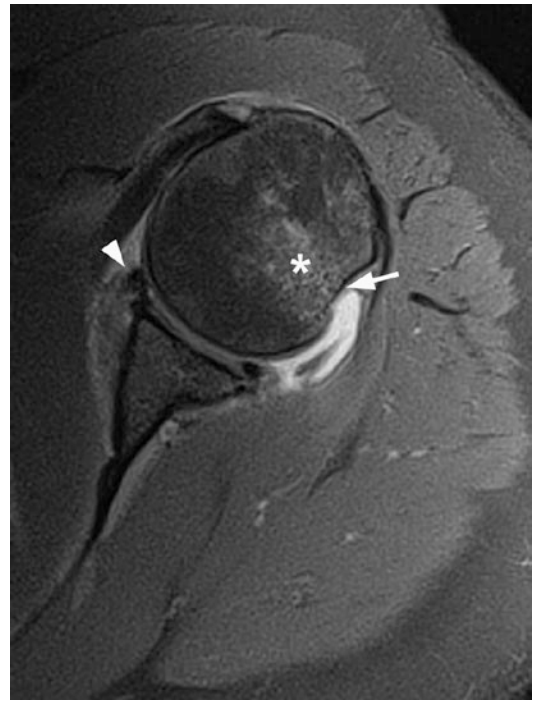

Fig. 14.20 Hill-Sachs lesion following anterior shoulder dislocation. Axial PD fs FSE MR image shows focal impaction of the posterior humeral head (arrow) with underlying edema-like marrow signal (asterisk) from recent contusion and the torn anterior labrum (arrowhead)

humeral head should appear circular. Clinicians should be aware, however, that there is a normal anatomic groove located posterolaterally and caudally on the humeral head; this groove should not be miscategorized as a Hill-Sachs lesion [40].

Posterior labral and capsular tears are less common than anterior tears and are usually seen in association with posterior or multidirectional instability. These tears have signal changes and appearances similar to those of anterior labral tears on MR imaging, but in a posterior location. Posterior dislocation may cause impaction of the anterior humeral head on the posterior glenoid, leading to a "trough sign" or "reverse Hill-Sachs" lesion.

Overhead repetitive motion or acute trauma can cause superior labral lesions, which usually present as nonspecific shoulder pain. Superior labral tears are usually centered at the biceps labral complex extending from anterior to posterior to the biceps anchor (i.e., SLAP lesions). SLAP lesions may extend inferiorly to involve the anterior labrum, posterior labrum, and/or the biceps anchor; they may also involve adjacent capsuloligamentous structures [41]. On arthroscopy, SLAP lesions have a reported prevalence of 3.9–11.8% [42, 43]. On MR imaging/MR arthroscopy, high signal (fluid on T2 or arthrographic contrast on T1) is usually found extending into the superior labrum and tracking into the labral substance and/or the biceps tendon (Fig. 14.21). SLAP tears must be differentiated from the normal variant of a sublabral foramen. Sublabral foramina usually appear smooth, extend medially paralleling the glenoid contour, and do not extend into the posterior-superior labrum. SLAP tears most often have irregular margins, extend laterally within the labrum toward the biceps tendon, and involve the posterior-superior labrum. Differentiating among the various types of SLAP tears with MR imaging may be challenging in some cases.

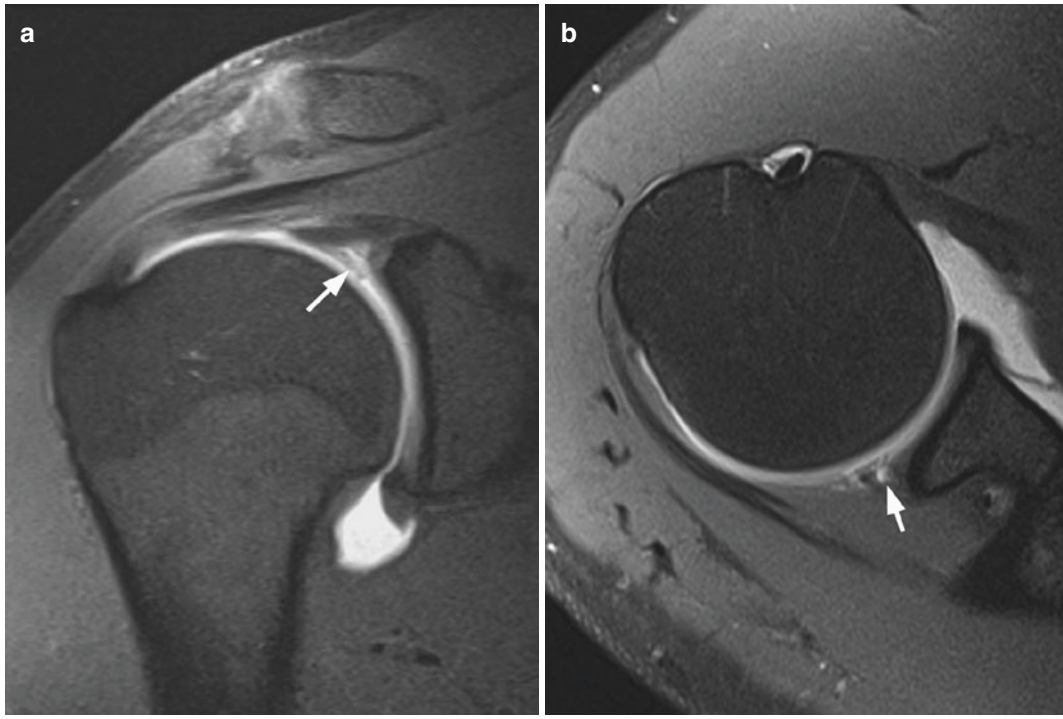

Fig. 14.21 Superior labral tear (SLAP). Coronal (**a**) and axial (**b**) T1W fs FSE images from an MR arthrogram show contrast beneath the labrum at the biceps anchor (**a**) and in the posterior labrum (**b**) (arrows)

Proximal tears of the long head of the biceps tendon, which are more common in patients aged more than 40 years, tend to be proximal to the bicipital groove of the humerus [44]. These tears appear on MR images as absence of the tendon at the biceps anchor since the torn end of the tendon retracts distally. There may be edema surrounding the biceps anchor and a fluid-filled tendon sheath. Because the tendon is "absent," the lesion may be easily overlooked, especially in the setting of massive rotator cuff tears; the intra-articular portion of the biceps tendon must be specifically identified on every shoulder MR image.

MR imaging can be used to assess pathologies of the rotator interval, the space between the supraspinatus and subscapularis tendons through which the long head of the biceps tendon courses. The rotator interval is the site of many biceps tendon lesions, adhesive capsulitis, and anterosuperior internal impingement [45]. Adhesive capsulitis, also known as frozen shoulder, is often idiopathic. Primary myofibroblastic transformation of tissues leads to contracture of the coracohumeral ligament component of the rotator interval [46]. A painful global limitation of both active and passive shoulder motion occurs in these patients [46]. On MR imaging, abnormal thickening and/or edema of rotator interval structures and the inferior glenohumeral ligaments and joint capsule can be seen (Fig. 14.22). Edema-like capsular signal around the glenoid rim may also be apparent on fat-suppressed MR images.

When insufficient information is available from radiographs in cases of complex osteoarthritis or inflammatory arthritis, MR imaging can be useful in demonstrating the changes of early disease, bony involvement, hyperplastic synovium, and treatment response. Rotator cuff tears and effusion-synovitis are also well demonstrated on MR images for these patients.

MR imaging also plays an important role in the diagnosis, characterization, assessment of extent, and treatment planning for bone and soft tissue tumors around the shoulder during preoperative

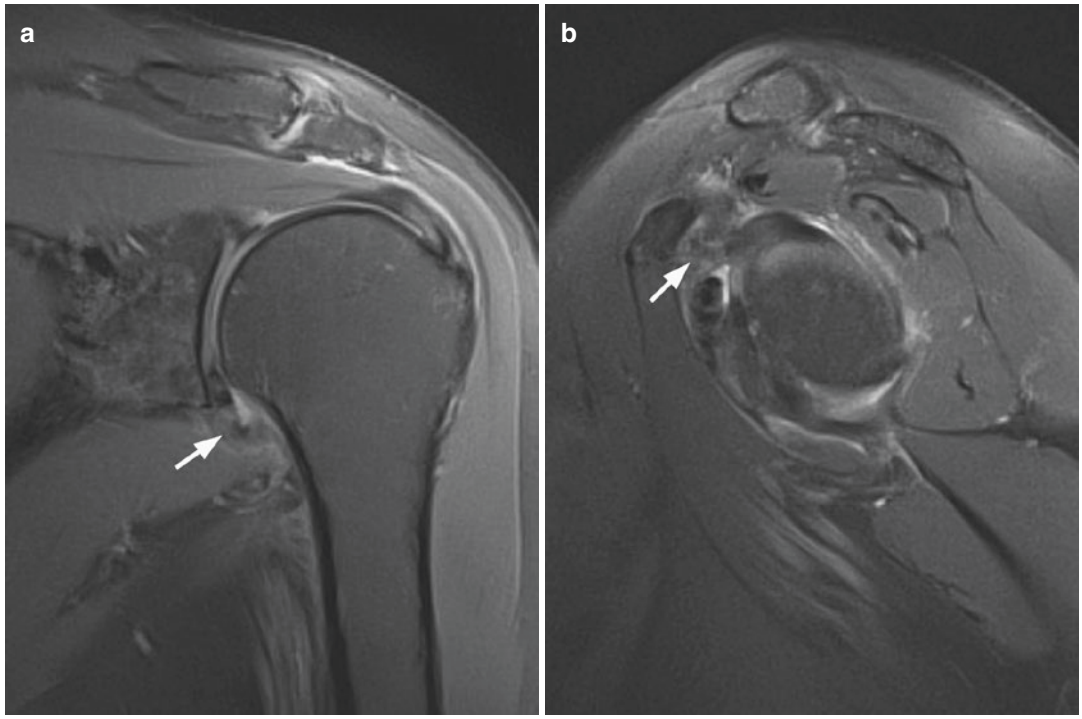

Fig. 14.22 Adhesive capsulitis. A coronal T2-weighted fs FSE image (**a**) with edema in and around the capsule in the axillary recess (arrow, **a**). Sagittal oblique T2-weighted fs FSE image demonstrates edema in the rotator interval (arrow, **b**)

evaluation. These tumors demonstrate wide variations in signal characteristics on MR images.

Finally, MR imaging is useful for evaluating infection of the shoulder, distinguishing between a fluid collection and inflammatory phlegmon, and identifying the occurrence of osteomyelitis via the presence of low subchondral bone marrow signal on non-fat-suppressed T1-weighted images. Following contrast administration, perisynovial edema, inflamed synovium, and soft tissue sinus tracts can be outlined by enhancement on fat-suppressed T1-weighted images.

14.5 Ultrasound

Ultrasound (US) imaging of the shoulder has the advantage of being a less expensive and more rapid and dynamic examination than MR imaging and is therefore commonly used to assess the rotator cuff and biceps for tendinopathy, tenosynovitis, tears, and calcific tendinitis [47]. However, labral tears including SLAP tears are better visualized by MR imaging because the interposed bone obscures portions of these structures on US images. Perhaps most importantly, US is an excellent modality to guide the use of nerve blocks; barbotage treatment of calcific tendinitis; therapeutic injections of the joints, bursae, and ligaments; and other interventions.

Proper performance of US examinations is operator-dependent and requires significant training and experience. The shoulder must be positioned appropriately for the structure or pathology that is to be evaluated. Several patient positions are required for a complete shoulder examination.

14.6 Conclusion

This chapter reviewed the imaging modalities commonly used to assess shoulder pathologies. Radiography, CT, MR, and US imaging are

complementary examinations that can provide vital information to clinicians in regard to treatment decisions, preoperative planning, and follow-up, including outcomes assessment and diagnosis of complications. A basic understanding of image interpretation is therefore essential for the optimal treatment of shoulder disorders.

Acknowledgment We thank our scientific medical writer, Megan Griffiths, MA, for her help with editing this book chapter.

References

1. Mitchell C, Adebajo A, Hay E, Carr A. Shoulder pain: diagnosis and management in primary care. BMJ. 2005;331(7525):1124–8.
2. Urwin M, Symmons D, Allison T, et al. Estimating the burden of musculoskeletal disorders in the community: the comparative prevalence of symptoms at different anatomical sites, and the relation to social deprivation. Ann Rheum Dis. 1998;57(11):649–55.
3. Shanahan EM, Sladek R. Shoulder pain at the workplace. Best Pract Res Clin Rheumatol. 2011;25(1):59–68.
4. Milgrom C, Schaffler M, Gilbert S, van Holsbeeck M. Rotator-cuff changes in asymptomatic adults. The effect of age, hand dominance and gender. J Bone Joint Surg Br. 1995;77(2):296–8.
5. Pandya J, Johnson T, Low AK. Shoulder replacement for osteoarthritis: a review of surgical management. Maturitas. 2018;108:71–6.
6. Court-Brown CM, Caesar B. Epidemiology of adult fractures: a review. Injury. 2006;37(8):691–7.
7. Karl JW, Olson PR, Rosenwasser MP. The epidemiology of upper extremity fractures in the United States, 2009. J Orthop Trauma. 2015;29(8):e242–4.
8. Roux A, Decroocq L, El Batti S, et al. Epidemiology of proximal humerus fractures managed in a trauma center. Orthop Traumatol Surg Res. 2012;98(6):715–9.
9. Simovitch R, Sanders B, Ozbaydar M, Lavery K, Warner JJ. Acromioclavicular joint injuries: diagnosis and management. J Am Acad Orthop Surg. 2009;17(4):207–19.
10. Mettler FA Jr. Essentials of radiology. 3rd ed. Albuquerque, NM: Saunders; 2013.
11. Nam D, Maak TG, Raphael BS, Kepler CK, Cross MB, Warren RF. Rotator cuff tear arthropathy: evaluation, diagnosis, and treatment: AAOS exhibit selection. J Bone Joint Surg Am. 2012;94(6):e34.
12. Axtell LM, Asire AJ, Myers MH, editors. Cancer Patient Survival. Report Number 5. Washington, DC: US Department of Health, Education and Welfare; 1976.
13. Dahlin DC. Bone tumors: general aspects and data on 6,221 cases. 3rd ed. Springfield, IL: Charles C Thomas; 1978. p. 156–75.
14. Rubin P. Clinical oncology: a multidisciplinary approach. 6th ed. Rochester, MN: American Cancer Society; 1983.
15. Dahlin DC, Ivins JC. Benign chondroblastoma. A study of 125 cases. Cancer. 1972;30(2):401–13.
16. Enneking WF. Simple cyst. In: Enneking WF, editor. Musculoskeletal tumor surgery. New York, NY: Churchill Livingstone; 1983. p. 1494–513.
17. Enneking W, Dunham W, Gebhardt M, Malawer M, Pritchard D. A system for the classification of skeletal resections. Chir Organi Mov. 1990;75(1 Suppl):217–40.
18. Gregory T, Hansen U, Khanna M, et al. A CT scan protocol for the detection of radiographic loosening of the glenoid component after total shoulder arthroplasty. Acta Orthop. 2014;85(1):91–6.
19. Gerber C, Pennington SD, Nyffeler RW. Reverse total shoulder arthroplasty. J Am Acad Orthop Surg. 2009;17(5):284–95.
20. Roche C, Flurin PH, Wright T, Crosby LA, Mauldin M, Zuckerman JD. An evaluation of the relationships between reverse shoulder design parameters and range of motion, impingement, and stability. J Shoulder Elb Surg. 2009;18(5):734–41.
21. Verhofste B, Decock T, Van Tongel A, De Wilde L. Heterotopic ossification after reverse total shoulder arthroplasty. Bone Joint J. 2016;98-B(9):1215–21.
22. Monga P, Funk L. Diagnostic clusters in shoulder conditions. Lancashire: Springer; 2017.
23. Castagno AA, Shuman WP, Kilcoyne RF, Haynor DR, Morris ME, Matsen FA. Complex fractures of the proximal humerus: role of CT in treatment. Radiology. 1987;165(3):759–62.
24. Delage Royle A, Balg F, Bouliane MJ, et al. Indication for computed tomography scan in shoulder instability: sensitivity and specificity of standard radiographs to predict bone defects after traumatic anterior glenohumeral instability. Orthop J Sports Med. 2017;5(10):2325967117733660.
25. Cook TS, Stein JM, Simonson S, Kim W. Normal and variant anatomy of the shoulder on MRI. Magn Reson Imaging Clin N Am. 2011;19(3):581–94.
26. McNally EG, Rees JL. Imaging in shoulder disorders. Skelet Radiol. 2007;36(11):1013–106.
27. Zlatkin MB, Iannotti JP, Roberts MC, et al. Rotator cuff tears: diagnostic performance of MR imaging. Radiology. 1989;172(1):223–9.
28. Palmer WE, Brown JH, Rosenthal DI. Rotator cuff: evaluation with fat-suppressed MR arthrography. Radiology. 1993;188(3):683–7.
29. Helms CA. Fundamentals of skeletal radiology. 4th ed. Durham, NC: Saunders; 2013.
30. Steinbach LS. MRI of shoulder instability. Eur J Radiol. 2008;68(1):57–71.
31. Mall NA, Kim HM, Keener JD, et al. Symptomatic progression of asymptomatic rotator cuff tears: a prospective study of clinical and sonographic variables. J Bone Joint Surg Am. 2010;92(16):2623–33.
32. Kim HM, Dahiya N, Teefey SA, Keener JD, Galatz LM, Yamaguchi K. Relationship of tear size and

location to fatty degeneration of the rotator cuff. J Bone Joint Surg Am. 2010;92(4):829–39.
33. Gladstone JN, Bishop JY, Lo IK, Flatow EL. Fatty infiltration and atrophy of the rotator cuff do not improve after rotator cuff repair and correlate with poor functional outcome. Am J Sports Med. 2007;35(5):719–28.
34. Galatz LM, Ball CM, Teefey SA, Middleton WD, Yamaguchi K. The outcome and repair integrity of completely arthroscopically repaired large and massive rotator cuff tears. J Bone Joint Surg Am. 2004;86-A(2):219–24.
35. de Jesus JO, Parker L, Frangos AJ, Nazarian LN. Accuracy of MRI, MR arthrography, and ultrasound in the diagnosis of rotator cuff tears: a meta-analysis. AJR Am J Roentgenol. 2009;192(6):1701–7.
36. Feldman F. Radiology of shoulder prostheses. Semin Musculoskelet Radiol. 2006;10(1):5–21.
37. Tirman PF, Steinbach LS, Feller JF, Stauffer AE. Humeral avulsion of the anterior shoulder stabilizing structures after anterior shoulder dislocation: demonstration by MRI and MR arthrography. Skelet Radiol. 1996;25(8):743–8.
38. Neviaser RJ, Neviaser TJ, Neviaser JS. Anterior dislocation of the shoulder and rotator cuff rupture. Clin Orthop Relat Res. 1993;291:103–6.
39. Neviaser RJ, Neviaser TJ, Neviaser JS. Concurrent rupture of the rotator cuff and anterior dislocation of the shoulder in the older patient. J Bone Joint Surg Am. 1988;70(9):1308–11.
40. Richards RD, Sartoris DJ, Pathria MN, Resnick D. Hill-Sachs lesion and normal humeral groove: MR imaging features allowing their differentiation. Radiology. 1994;190(3):665–8.
41. Chang D, Mohana-Borges A, Borso M, Chung CB. SLAP lesions: anatomy, clinical presentation, MR imaging diagnosis and characterization. Eur J Radiol. 2008;68(1):72–87.
42. Snyder SJ, Banas MP, Karzel RP. An analysis of 140 injuries to the superior glenoid labrum. J Shoulder Elb Surg. 1995;4(4):243–8.
43. Maffet MW, Gartsman GM, Moseley B. Superior labrum-biceps tendon complex lesions of the shoulder. Am J Sports Med. 1995;23(1):93–8.
44. Stoller DW. Magnetic resonance imaging in orthapaedics and sports medicine. 3rd ed. Philadelphia, PA: Lippincott Williams & Wilkins; 2007.
45. Lee JC, Guy S, Connell D, Saifuddin A, Lambert S. MRI of the rotator interval of the shoulder. Clin Radiol. 2007;62(5):416–23.
46. Bunker TD, Anthony PP. The pathology of frozen shoulder. A Dupuytren-like disease. J Bone Joint Surg Br. 1995;77(5):677–83.
47. Michelin P, Legrand J, Lee KS, et al. Axillary sonography of the shoulder: an adjunctive approach. J Ultrasound Med. 2018;37(11):2707–15.